SEMARAK ILMU PUBLISHING

Journal of Advanced Research in Fluid Mechanics and Thermal Sciences

Journal homepage:
https://semarakilmu.com.my/journals/index.php/fluid_mechanics_thermal_sciences/index
ISSN: 2289-7879

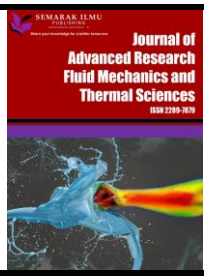

Improve the Performance of Integrated Collector Storage-Solar Water Heater by using Glazing Confined Air Space: A Numerical Simulation Approach

Angham Fadil Abed[1], Noora A. Hashim[1,*], Rasha Hayder Hashim[1]

[1] Department of Mechanical Engineering, Faculty of Engineering, University of Kufa, Al-Najaf Governorate, Iraq

ARTICLE INFO

Article history:
Received 9 August 2023
Received in revised form 26 October 2023
Accepted 9 November 2023
Available online 30 November 2023

Keywords:
Solar heater; CFD analysis of integrated collector storage-solar water heater; performance of integrated collector storage-solar water heater; thermal efficiency

ABSTRACT

A numerical study is presented by double-glazed the conventional rectangular integrated collector storage-solar water heater with internal obstacle in the storage container which improving the performance and making them convenience for household uses. A three-dimensional, laminar and unsteady numerical simulation with the aiding of COMSOL 5.5 software is used to investigate three shapes of integrated collector storage-solar water heaters (single glazed, double glazed, and double glaze-obstacle). The governing equations which represented of conservation equations of mass, momentum and energy. The performance of these systems was tested along two days in February and July during different atmospheric conditions at Kufa-Iraq. In these days, the water temperature reached a maximum value of 61.02 ℃ for no-load condition when the tap temperature was 39.3℃. Obstacle and glazed integrated collector storage –solar water heater shows the higher performance as compared with the two other heaters with a maximum value of instantaneous efficiency of 59.95 % in February.Also, the average Nusselt number and heat transfer between the absorber plate and confined air decreases and this increase a storage water temperature. In general, the total efficiency under no-load conditions is lower than on load case. The results were compared to previous theoretical and experimental work and show a good agreement with a maximum error that not exceeds to (4.24 %).

1. Introduction

The world's energy supply must improve its sustainability in the future. This can be accomplished by using energy more wisely and depending on renewable energy sources, including wind, hydropower, solar, and geothermal energy [1]. The most fundamental renewable energy source found in nature is solar energy that enters the planet. One of the most significant positions among the numerous alternative energy sources is held by solar energy [2]. Solar energy technologies are crucial elements of a sustainable energy future since they provide a home, clean, and renewable energy source [3]. A large energy demands for cooling, heating and other domestics or industrial

* *Corresponding author.*
E-mail address: nooraa.alkhalidi@uokufa.edu.iq

https://doi.org/10.37934/arfmts.111.2.4364

requirements are made the energy conservation is a major suitable solution for a huge problem. Solar water heaters are the most common solution to overcome this problem. Solar radiation is converted by SWHs into thermal energy that heats the heat transfer fluids inside which is usually water [4-6]. Solar water heaters can be considered as the fastest and widest developing techniques within the renewable energy technologies [7]. In areas of lack electricity supply with abundance sunlight a small water heater may consider as an economic and a practical device resource of hot water for many years. A novel and eco-friendly method of heating structures worldwide is made possible by solar water heating and solar source heat pumps. As a result, these technologies can be employed to reduce air emissions and negative effects on the environment [8]. As they may utilize renewable heat sources found in our environment, they provide the most energy-efficient solution to supply heating and cooling in many applications [5,6]. SWHs are classified commonly to three subdivisions as: natural (free) and forced convection solar water heaters, and finally (under study type) the Integrated Collector-Storage Solar Water Heater (ICSSWH) which are the cheapest and simplest design due to be free of moving parts [9,10].

The built-in- ICSSWH has a lot of advantages over the other types. Firstly, the efficiency during the daytime is high because there are no high heat losses due to water circulation. Secondly, it has a better heat transfer because of the large area of contact between the water and absorber plate if it compared with the poor bond conductance in case of forced and natural convections types. Finally, it is manufactured from low cost materials and by easy manufacture ways without the need for high technologies ways [11]. Several researches were implemented in many parts of the world that aimed to improve (ICSSWH) performance by discussing a variety of designs. A new design of solar water heater was suggested by Garg [12]. A 90 liters capacity storage SWH was constructed by rectangular tank of a 112*80*10 cm dimensions. It performed a dual function of the heat absorption and heated water stored. The performance tests were investigated at Johdpur (Latitude 26.3 N) in India. Results showed 90 liters of water at 50 to 60 ℃ mean temperature in winter while 60 to 75 ℃ in summer which measured at 4:00 p.m. could be supplied. It was also indicated that a sufficient hot water could be obtained in the early morning if the heater was covered with a blanket as an insulation overnight or in case of the hot water was stored in an insulated tank. A performance equation for this solar water heater was also developed. The optimum distance between the lower and upper plate of the heater was found to be 10 cm. Sodha *et al.,* [13] presented an improved analysis of a collector and storage solar water heater arrangement which consisted of an insulated rectangular tank measuring (1.22*0.9*0.2) m with its top surface suitably blackened and covered with glass. In this system the collector acted as a storage tank. It was found that after the collection of solar energy during a day, heater could store a substantial amount of heat for an appreciable time if the top glass sheet is covered by a suitable insulation through night. Analytical expressions for transient temperature of water were derived and their results were found to be in good agreement with the hourly-recorded temperature of water in the tank collector.

A low cost collector storage solar water heater SWH had been developed by Nahar and Malhotra [14]. It consisted of a rectangular galvanized steel tank of dimensions 1.12*0.8*0.1 m having a capacity of 90 liters, the heater was inclined at 41 o to the horizontal and facing south during the winter season. Also, it was found that inserting of an insulating cover at night, the water remained warm till next morning. Abd-Alghani [15] investigated experimentally the performance of two domestic solar water heaters under natural and forced convection. The natural convection system consisted of a flat-plate collector of 1.5 m^2 absorber area and storage tank of capacity of 125-liters. For both cloud clear and cloudy weather conditions in summer and winter experiments were achieved. The system performance was evaluated hourly for all test conditions. To find the contribution of solar energy in domestic hot water supply, the final mean tank temperature was

measured daily in Basrah, Iraq (latitude 30.76 °N) and tests were done. For Loading conditions continuous intermittent and load was imposed and the system performance was investigated for each condition. The maximum temperature was 65 ℃ while the inlet temperature was 35℃. Garge and Rani [16] studied theoretically and experimentally the effect of using an insulated baffle plate inside the tank adjacent to the absorber plate and also using of an insulation cover during cooling hours. The tested solar water heater consisted of a rectangular galvanized steel tank of dimensions 1.12*0.8*0.1 m having a capacity of 90 liters. The heater was inclined °45 from horizontal at Delhi and was oriented due south in the winter season. Theoretical study was done by the analysis of mathematical model contained from unsteady energy equations; the performance of the system was predicted by solving the model equations numerically by finite difference technique. An improvement of 70% could be achieved by using the insulation cover. Using of a baffle plate improves the performance during the day conventional systems. In addition, the experimental results were in agreement with theoretical predictions. Using the ANSYS program, Khalifa and Mehdi [17] performed a numerical and an experimental study on storage tank of thermosiphon SWHs. It was found that temperature gradients in radial and axial direction were negligible compared to the temperature in the vertical direction. Also, the average storage temperature can be calculated from the vertical distribution at tank center. Farhan [18] studied numerically the performance of a prism shaped storage solar collector with a right triangle cross sectional area by using ANSYS software. The performance parameters used were collector temperature, mean tank temperature, velocity distribution, total energy stored and the best outlet and inlet water flow locations. A good agreement was achieved by Farhan [18] when it compared with the theoretical results available in the literatures at that time. Vaxman and Sokolov [19] Investigated experimentally and analytically the design of an integral compact SWH. A built-in collector and water tank were used with water flow caused by thermosphonic force. Two systems geometry were analyzed. The results obtained proved that the efficiency of the modified design was best. Additionally, the theoretical ANSYS analysis agreed with experimental results. Joudi *et al.,* [20] investigated effectiveness of a rectangular solar collector. Without partition, average water temperature reached in the winter and summer was 37 °C and 46 °C, respectively. The results showed that applying the barrier can improve the storage collector's performance as well as night time. Also, it was found in case of the baffle plate system that was covered with insulation during night, it sufficiently hots water up to 55°C in the early morning hours can be supplied. Pandya and Behura [21] studied the thermal performance of a V-Through SWH. The device was constructed in Jaipur, India, to support various tilt degrees. When the tilt angle was changed from 15° to 25°, the system's thermal efficiency improved from 27% to 30%. Ahmad *et al.,* [22] conducted an experimental and numerical investigation on a storage solar collector to determine its viability for home usage. In the article was a study on the impact of the front absorber plate's surface shape wavy, flat, and zigzag on the efficiency of storing solar collectors. This was done by building built-in water heaters of the three-box type. Compared to the wavy and flat plate collectors, the zigzag plate collector performed better.

In the study of Ambarita *et al.,* [23], the relationship between the inclination angle and the flat plate solar collector's performance is examined. To investigate the fluid flow and heat transfer properties in the enclosure, numerical simulations utilizing commercial Computational Fluid Dynamic (CFD) software have been conducted. The inclination angle's impact on the collector's performance has been demonstrated. As the inclination angle increases, the average heat transfer coefficient drops.

Abdullah *et al.,* [24] investigate experimentally a new design of integrating solar cell technology and the solar storage collector into one system (PV)/storage solar collector. The results showed that the outlet water temperature reaches the maximum value of 42°C at 2 PM for the PV/storage

collector at spring day, and the temperature differences between the outlet and inlet temperature are 14.6^{o}C and 30^{o}C at 2 PM for the PV/storage collector and the conventional storage collector, respectively.

Experimental research on the performance of ICS-SWHs paired with a reflector-insulator cover is done by Mokhlif *et al.,* [25]. The reflectors included insulation on the back so that they could double as covers at night and reflectors during the day. The findings showed that, when compared to the ICS-SWH without insulated reflectors, the thermal efficacy of the latter was increased by 23%. Additionally, the maximum temperature of the water that is stored reaches 46 °C in the morning of the coldest day and 82 °C during the day.

To determine the ideal circumstances for operating in the mode of discharge, Chandra and Matuska [26] created a variety of CFD models and experimentally validated them on a test rig of a nearby hot water storage tank. In order to break up stratification, cold and hot water were mixed vigorously in this experiment. The governing equations of the fluid flow in a tank were solved using the Fluent-ANSYS19.2 model. The numerical findings demonstrated that the tank's operating conditions can be enhanced by wisely choosing the inlet device. According to the study's findings, storage tanks with built-in heaters might be made more efficient and used with heat pumps or solar energy systems.

Experimental research on an ICS-SWH system with a dual glazing cover and a corrugated absorber plate was conducted by Mokhlif *et al.,* [27]. Investigations were done into how the dual glazing cover affected the performance of the ICS-SWH. On the first morning of the second and third days, it was discovered that storage water temperatures in scenarios with dual glazing covers were 6 and 11 degrees Celsius higher than those in situations with single glazing covers. The built-in regime's average daily thermal efficacy was 68% and its mass flow rate was 0.0091 kg/s. The daily thermal efficacy under a dual-glazing cover was 4.6% higher than under a single-glazing cover.

An ICS-SWH system with a corrugated absorber plate and a single glazing cover was experimentally studied by Yassen *et al.,* [28]. On the coldest day in January that Iraq could have experienced, the final temperature of the water that had been stored was 59 °C. It was discovered that the temperature of the stored water was higher than for the previous examination, which was mostly due to the corrugated absorber in the storage tank.

After reviewing the aforementioned literature, it was discovered that there had been little research on the effects of additional glass cover with a closed air space for the rectangular Integrated Collector-Storage (ICS) solar water heater. Accordingly, the main objective of the current study focused on improving the performance of the rectangular ICS heater by using two glazed panels' covers to show its viability for home use using a three-dimensional, unsteady model. The inclusion of a double glass cover lessens heat transfer to the surroundings. The second objective of this research project is to examine how the operational parameters of the heater are affected by internal obstructions and environmental variables.

2. Research Methodology

2.1 Description of the ICS Heater

The physical arrangements of a rectangular storage solar water heater in three dimensions (3-D) are shown in Figure 1(a), Figure 1(b), and Figure 1(c). (single glazed ICS solar heater) is used in the first arrangement; the (double glazed ICS solar heater) in the second and is constituted mainly of a single glazed ICS heater with additional glass cover over the heater with an enclosed air space of depth 0.02 m, and an internal (double glaze-obstacle ICS solar heater) in the third. For all arrangements, cold water enters the heater through an intake at the bottom in all models. Hot water

with lesser density rises to the top of the heater when the sun warms the sloped absorbent surface. When the outlet at the top of the heater is opened, hot water flows and another cold water enters through the bottom intake and this case is termed as load condition [29,30] , while no load case occur when the outlet hot water at the top of the heater is closed, hot water isn't flows or withdrawing. The absorber plate's distance from the glass bottom surface, which sloped upward by 45 degrees, was maintained at 45 mm, which is at the acceptable range for solar collectors [31]. The ICS heaters inclined at angle of 30^o which is approximately the latitude of Kufa, in order to collect a maximum solar energy. The walls, both vertical and horizontal, were insulated.

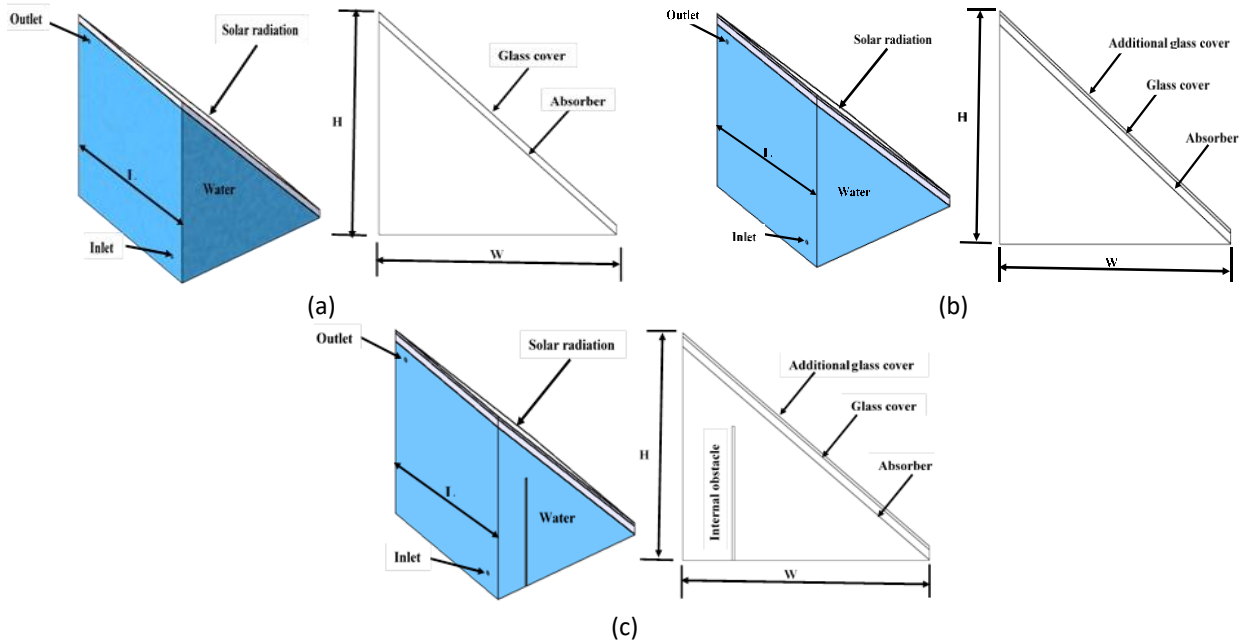

Fig. 1. Schematic of the ICS heaters; (a) Single glazed ICS heater, (b) Double glazed ICS heater and (c) Double glaze-obstacle ICS heater; configurations

2.2 Governing Equations and Boundary Conditions

For Boussinesq approximation, the fluid is taken as incompressible and Newtonian, which means fluid density is assumed to be constant except for calculating the effect of density changes in buoyant forces. Density is slightly varied only with temperature. With these assumptions characteristic of free convection and the buoyant effects are included as body forces in the equations of momentum. Therefore, the properties of water were considered to be temperature dependent. Three dimensional unsteady laminar fluid motion is assumed because of very low velocity within the collector storage with no internal heat generation with neglecting the effect of viscous energy dissipation. The vertical and horizontal walls were insulated [32].

Equation of Continuity:

$$\frac{\partial \rho}{\partial t} + \frac{\partial u}{\partial x} + \frac{\partial v}{\partial y} + \frac{\partial w}{\partial z} = 0 \tag{1}$$

where
u = velocity in x-direction (m/s)
v = velocity in y-direction (m/s)
w = velocity in z-direction (m/s)
ρ = density of flow [kg/m^3]

Momentum equations [28]:

In x-direction:

$$\rho\left(\frac{\partial u}{\partial t}+u\frac{\partial u}{\partial x}+v\frac{\partial u}{\partial y}+w\frac{\partial u}{\partial z}\right)=\rho g_x-\frac{\partial P}{\partial x}+\mu(\frac{\partial^2 u}{\partial x^2}+\frac{\partial^2 u}{\partial y^2}+\frac{\partial^2 u}{\partial z^2}) \quad (2)$$

In y-direction:

$$\rho\left(\frac{\partial v}{\partial t}+u\frac{\partial v}{\partial x}+v\frac{\partial v}{\partial y}+w\frac{\partial v}{\partial z}\right)=\rho g_y-\frac{\partial P}{\partial y}+\mu(\frac{\partial^2 v}{\partial x^2}+\frac{\partial^2 v}{\partial y^2}+\frac{\partial^2 v}{\partial z^2}) \quad (3)$$

In z-direction:

$$\rho\left(\frac{\partial w}{\partial t}+u\frac{\partial w}{\partial x}+v\frac{\partial w}{\partial y}+w\frac{\partial w}{\partial z}\right)=\rho g_z-\frac{\partial P}{\partial z}+\mu(\frac{\partial^2 w}{\partial x^2}+\frac{\partial^2 w}{\partial y^2}+\frac{\partial^2 w}{\partial z^2}) \quad (4)$$

where
P = pressure of fluid [Pa]
μ = viscosity of fluid dynamic [N.s/ m^2]

Equation of Energy [28]:

$$\rho C_p(\frac{\partial T}{\partial t}+u\frac{\partial T}{\partial x}+v\frac{\partial T}{\partial y}+w\frac{\partial T}{\partial z})=K(\frac{\partial^2 T}{\partial x^2}+\frac{\partial^2 T}{\partial y^2}+\frac{\partial^2 T}{\partial z^2}) \quad (5)$$

where
C_p = specific heat of fluid [J/kg K]
K = thermal conductivity of fluid [W/m.K]

As a function of water temperature, the physical-thermal properties of water are listed in Table 1 [33]. The boundary conditions are:At the inlet: water enters with a constant mass flow rate and changeable inlet temperature $\mathrm{T_{in}(t)}$.

Table 1
Water thermo-physical properties [29]

Quantity	Expression
Density(kg/m^3)	$\boldsymbol{\rho = 1001 - 0.08832 * T - 0.003417 * T\text{^}2}$
Specific heat (J/kg.K)	$\boldsymbol{C_p = 4226 - 3.224 * T + 0.0575 * T\text{^}2 - 0.0002656 * T\text{^}3}$
Thermal conductivity (W/m K)	$\boldsymbol{K = 0.557 + 0.002198 * T\text{^}1 - 0.00000708 * T\text{^}2}$
Kinematic viscosity (m^2/s)	$\boldsymbol{\nu = (\frac{1}{0.5155+0.0192T} + 0.12) * 10\text{^} - 6}$

At the top plate, which is the clear additional glass cover, solar radiation flux $\mathrm{I(t)}$ is applied and changes during the simulated days, and external exchanges between the transparent cover and outside air are convective equal to $\mathrm{Q_{cam}}$ and radiative equal to $\mathrm{Q_{rsk}}$ (see Figure 2) where [34,35];

$$Q_{cam} = h_{cam}(T_{ag} - T_{am}) \tag{6}$$

$$h_{cam} = 2.8 + 3.3\mathrm{v_{wi}} \tag{7}$$

$$Q_{rsk} = 0.9 \times \sigma \times \varepsilon \times (T_{ag}^4 - T_{sk}^4) \tag{8}$$

where
h_{cam} = convective heat transfer coefficient to ambient [W/m^2.K]
T_{ag} = additional glass cover temperature [^{o}C]
T_{am} = ambient temperature [^{o}C]
σ = Stefan-Boltzmann constant
T_{sk} = Sky temperature [^{o}C]
$\mathrm{v_{wi}}$ = wind velocity [m/s]

The following is the formula used by Swinbank [36] and Saleh [37] to represent the external sky temperature $\mathrm{T_{sk}}$:

$$T_{sk} = 0.0552T_{am}^{1.5} \tag{9}$$

Heat flux equal to $\mathrm{Q_{ag}}$ is applied at top surface of additional glass cover for double glazed ICS heater, and double glaze-obstacle ICS heater. Heat flux equal to $\mathrm{Q_g}$ is applied at the top of the glass cover for all models. Heat flux equal to $\mathrm{Q_{absor}}$ is applied at top of the absorber plate (see Figure 2). At the horizontal and vertical walls, which are designated as an "adiabatic wall". Impermeable boundary and no-slip wall conditions have been implemented. For solid boundaries of fluid domain: u, v, w = 0, For outlet: p = 0. The initial Conditions are implemented at t= zero and can be written as:

$$u, v, w = 0 \tag{10}$$

$$P(x, y, z, 0) = 0 \tag{11}$$

$$T(x, y, z, 0) = T_{in}(x, y, z, 9A.M) \tag{12}$$

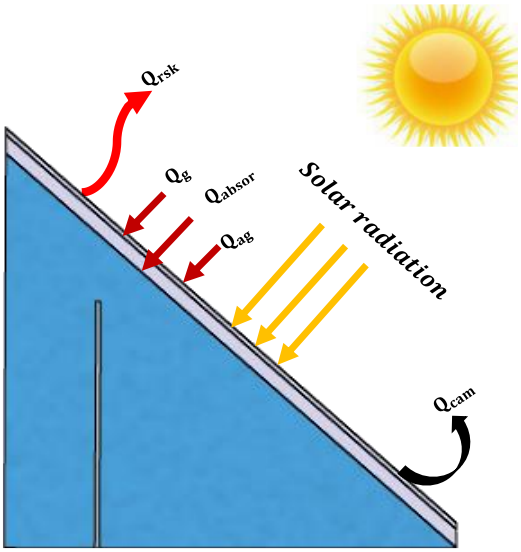

Fig. 2. Heat transfer types in ICS heater

3. Three-Dimensional Model

3.1 Meshing and Grid Test

Three-dimensional analysis of free convection is difficult because in addition to the energy equation three non-linear momentum equations must be solved. The boundary conditions are much more complicated than for two- dimensional convection. Therefore, it is suggested to employ the COMSOL Multiphysics to carry out the numerical investigation of the ICS heater. To solve the partial differential equations of changeable systems across time, the COMSOL 5.3 multiphasic program is much more practical and effective [38]. For numerical simulations, a three-dimensional, unsteady ICS solar heaters with dimensions of [length H of 1 m, width W of 1 m, and depth Z of 1 m] is developed in COMSOL. The solution is considered to be fully converged when the values of normalized residuals for each flow equation are smaller than a prescribed value of 10^{-3} except the energy equation of 10^{-4}. The model geometry of ICS solar heaters along with its meshes is shown in Figure 3 .The type of element employed in the current numerical model is free triangular and free tetrahedral shapes. A grid independence test has been done to check the mesh size for the models at a flow rate of 12 l/h. Different kinds of non-uniform grid systems are examined, and the storage fluid temperature is selected as the monitoring parameter. Although the difference in time is unacceptable, it is observed that the average storage temperature do not significantly alter between grid 4 and grid 5 meshing for (double glazed ICS heater) and (double glaze-obstacle ICS heater), or between grid 3 and grid 4 meshing for (single glazed ICS heater). Therefore, domain elements with (985393, 1517461 and 197809) respectively are taken into consideration for (double glazed ICS heater), (double glaze-obstacle ICS heater) and (single glazed ICS heater) in the numerical analysis. Table 2 shows the grid test results.

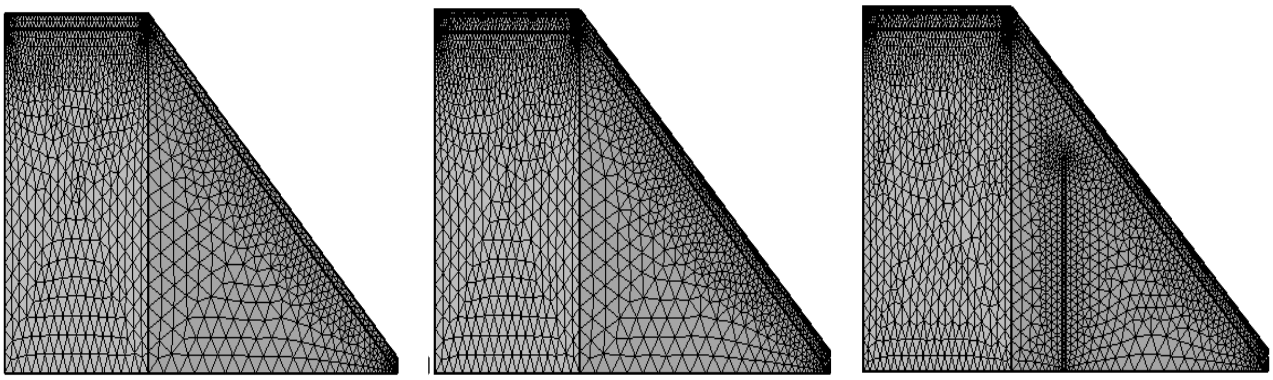

(a) (b) (c)

Fig. 3. Mesh of the ICS solar heaters; (a) Single glazed ICS heater, (b) Double glazed ICS heater, (c) Double glaze-obstacle ICS heater

Table 2
Characteristics of the tested meshes

Mesh size	Single glazed ICS heater			Double glazed ICS heater			Double glaze-obstacle ICS heater		
	Domain elements	Boundary elements	Edge elements	Domain elements	Boundary elements	Edge elements	Domain elements	Boundary elements	Edge elements
Grid 1	35404	7342	553	57226	12418	925	72376	14644	1112
Average storage temperature (^oC)	19.0043			24.617			24.921		
Grid 2	76018	13822	758	118419	23420	1295	151136	27200	1542
Average storage temperature (^oC)	19.9345			24.9087			25.4218		
Grid 3	197809	28420	1030	303994	50883	1974	426848	59587	2367
Average storage temperature (^oC)	20.2315			25.6267			25.9831		
Grid 4	719366	82802	1663	985393	125293	2514	1517461	148045	3262
Average storage temperature (^oC)	20.2320			26.3652			26.9762		
Grid 5				8131526	711366	5525	8848105	740447	6357
Average storage temperature (^oC)				26.3643			26.9767		

3.2 Model Validation

The numerical simulation was validated with the experimental results of Al-Jubori [39] and numerical results of Alawi [40], for single glazed ICS heater. The results were shown in Table 3. The two additional ICS heaters weren't validated because there was no data to use. For this validation setup, the climatic conditions of the experimental study are used in our 3D simulation model to evaluate and compare the storage water temperature of the heater [39]. Table 3 makes it clear that the mean storage temperature reaches its maximum value at the end of the day, which is consistent with the findings of Alawi [40], with a mean absolute percent error (MAE) is 4.24 %. In contrast, the storage mean temperature reaches for maximum value before beginning to decline after 3 p.m., according to the findings of the experiment by Al-Jubori [39], with (MAE) of 3.82 %. There is good agreement between present simulation model and pervious results.

Table 3
Validation of storage temperature and the mean absolute error for the single glazed ICS heater with pervious results

Time(h)	Solar radiation	Water storage temperature (°C)		
		Present result - single glazed ICS heater	Experimental results [39]	Numerical results [40]
9	600	13.5	13.5	13.5
10	800	14.434	15.3	15.5
11	963	15.99	16.9	17.1
12	1020	17.9933	18.7	18.99
13	1000	20.09	20.6	20.8
14	910	21.1	22	22.229
15	750	22.26	22.8	23.392
16	480	23.51	22	24
MAE%		Simulation results of the present model with experimental results [39]	Simulation results of the present model with numerical results [40]	
		3.82	4.24	

3.3 Performance Calculation of ICS Heaters
3.3.1 Stored energy

The output useful energy of an ICS solar heater in case of no load condition (Q_{us_noload}) can be calculated from the equation [41]

$$Q_{us\_noload} = m_w C_w (T_f - T_s) \tag{13}$$

The heat collected by the system with load conditions (Q_{us_load}) was estimated from the following equation [42]:

$$Q_{us\_load} = \dot{m}_w C_w (T_{out} - T_{in}) + m_w C_w (T_f - T_s) \tag{14}$$

where
$\dot{m}_w$ = mass flow rate of water [kg/s]
m_w = mass of water in the heater [kg]
T_{out} = outlet temperature of load water from heater [°C]
T_{in} = inlet temperature of load water to heater [°C]
T_f = water temperature of the heater at end hour (without load) [°C]
T_s = water temperature of the heater at the beginning of hour (without load) [°C]
C_w = specific heat of water [J/kg K]

3.3.2 Instantaneous and overall efficiency

The instantaneous efficiency $\boldsymbol{\eta_{ins}}$ of a collector is simply the ratio of the useful delivered to the total incoming solar energy $\boldsymbol{I}$ or [43]:

$$\boldsymbol{\eta_{ins}} = \frac{\boldsymbol{Q_{us}}}{\boldsymbol{A_a . \tau_g . \alpha_{absor} . \sum I}} \tag{15}$$

The bulk or overall system efficiency $\boldsymbol{\eta_d}$was calculated based on [39,44]:

$$\boldsymbol{\eta_d} = \frac{\boldsymbol{m_w C_w (T_{av} - T_i)}}{\boldsymbol{A_a \tau_g \alpha_{absor} t_r \sum I}} \quad (16)$$

where
$\boldsymbol{A_a}$ = area of the absorber inclined surface [m^2]
$\boldsymbol{\tau_g}$ = transmissivity of glass cover [-]
$\boldsymbol{\alpha_{absor}}$ = absorber plate absorption coefficient [-]
t_r = operation period [s]
T_{av} = average water temperature [^{o}C]

3.3.3 Nusselt number

The relationship for Nusselt number $\mathbf{Nu}$ between two rectangular plates of confined air space for a tilt angles $\boldsymbol{\theta}$ from 0 to 75 is [45]:

$$\boldsymbol{Nu} = \mathbf{1} + \mathbf{1.44}\left[\mathbf{1} - \frac{\mathbf{1708}}{\boldsymbol{RaCos\theta}}\right]\left[\mathbf{1} - \frac{\mathbf{1708}(\boldsymbol{sin1.8\theta})^{\mathbf{1.6}}}{\boldsymbol{RaCos\theta}}\right] + \left[\left(\frac{\boldsymbol{RaCos\theta}}{\mathbf{5830}}\right)^{\mathbf{1/3}} - \mathbf{1}\right] \quad (17)$$

Where the meaning of the (+) exponent is that only positive value of the terms in the square brackets are to used (use zero if the terms is negative). Where Ra is Rayleigh number and can be calculated as [45]:

$$\boldsymbol{Ra} = \frac{\boldsymbol{g\beta\Delta T {t_a}^3}}{\boldsymbol{\vartheta\alpha}} \quad (18)$$

where
g = gravitational acceleration [m/s^2]
$\boldsymbol{\beta}$ = Coefficient of thermal expansion [K^{-1}]
$\boldsymbol{t_a}$ = thickness of confined air space [m]
α = Water thermal diffusivity [m^2/s]
ΔT = temperature difference [^{o}C]

The coefficient of convective heat transfer between the absorber and confined air ($\boldsymbol{h_{ab-conf.air}}$) can be given as:

$$\boldsymbol{h_{ab-conf.air}} = \frac{\boldsymbol{NuK_{air}}}{\boldsymbol{t_a}} \quad (19)$$

4. Results and Discussion

The numerical simulation is performed on selected clear days with operating weather conditions on Kufa -Iraq (32°N latitude) through (11th, of July) and (21st, of February) using withdrawal pattern with a total hot water use are 12 l/h. The parameters of the system performance are done methodically for all test conditions hourly. These included the outlet water and the mean storage temperatures, total stored energy and velocity distribution. The results will be presented in this paper for the three ICS solar heaters at no load and load conditions.

4.1 Weather Conditions

The variation of the intensity of solar radiation and ambient air temperature in July and February from 9:00 AM to 16:00 PM is shown in Figure 4. The temperature is seen to trend in the same direction as the solar irradiation. They rise in the morning, peak between 14 and 15 PM, and then start to decline in the late morning and early afternoon. It is important to note that this delay between the peak solar intensity and the peak ambient air temperature can be explained by the thermal capacity of the surrounding air as well as other elements like air density, moisture, quality, and so on. The highest ambient temperature was recorded in July at about 46.9°C. The figure also shows peaks of solar irradiance at about 12.0 PM for both tested days with a maximum value of 907 W/m^2. The average wind speed in July and February was 0.3 m/s and 0.7 m/s, respectively.

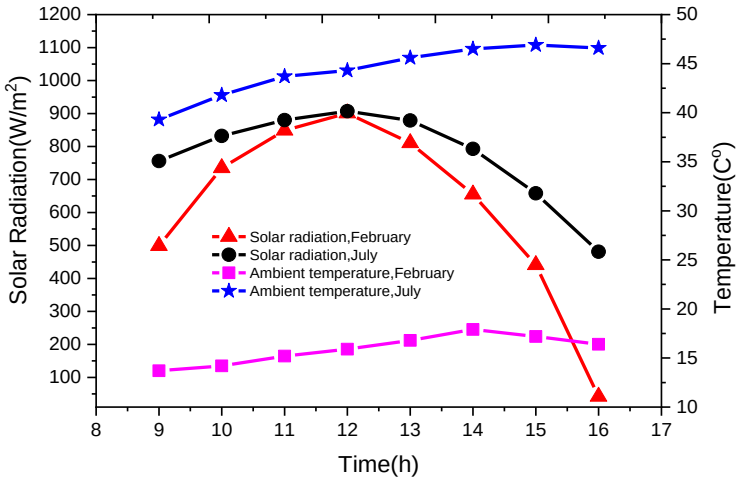

Fig. 4. Variation of weather conditions on July and February on Kufa-Iraq

4.2 Average Storage and Outlet Temperatures

Figure 5 shows the variation of the mean storage temperature during a specific day in February and July for no load condition. An increase in the mean storage temperature with time until the end of the operating period is noted. In July and February, the double glaze-obstacle ICS heater can warm up the water to a maximum storage temperature of (61.02 ℃ and 33.63℃ respectively) at 4 P.M when the tap water temperatures were (39.3 ℃ and 13.7℃ respectively) as compared to (49.64 ℃ and 22.93 ℃respectively) for single glazed ICS heater. From the figure, it can be seen there is a very small difference in storage temperatures between (double glazed ICS heater) and the (double glaze-obstacle ICS heaters.

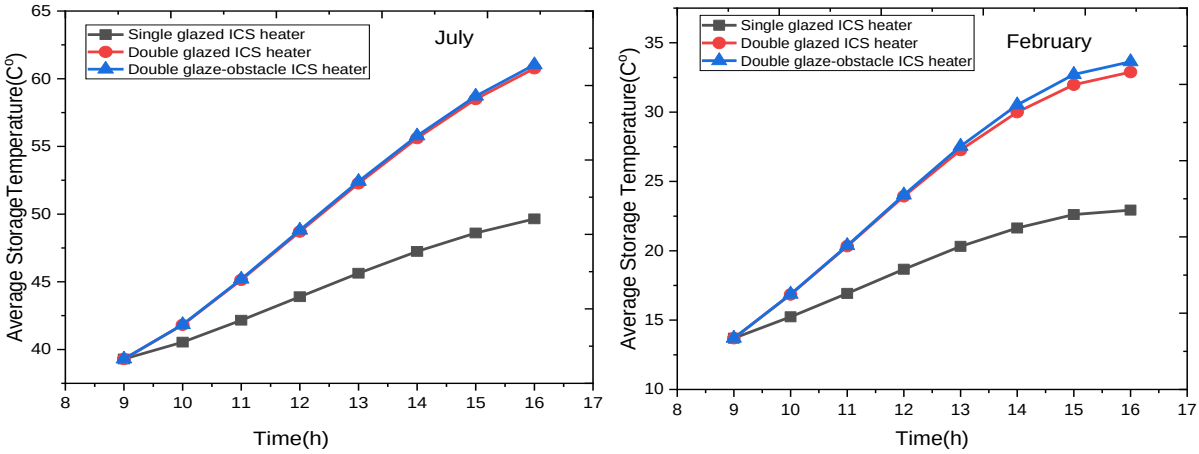

Fig. 5. Average storage temperature variation in case of no load condition in July and February

A simulation of continuous water flow (load condition) through the three ISC heaters was also conducted. Hot water was drawn continuously from the heaters. This was achieved by allowing the cold water enters the heater from the bottom and withdrawing hot water from heater top. The variation of average outlet, inlet and storage water temperatures in July and February for tests of volume flow rate of 12 l/h are shown in Figure 6 and Figure 7. The outlet and storage temperatures follow a similar behavior as inlet water temperature. It is noted that throughout the period between 9 a.m. and 3 p.m., the outlet and the mean storage temperatures are increasing, which means that the useful energy ($\mathbf{q_{us}}$) is higher than that carried out by water. A decreasing of these temperatures is started after 3 p.m because the value of useful energy becomes lower than the energy carried out by the water. The maximum difference between outlet and inlet water temperatures is 15.87 ° C in February at 3 p.m. for the (double glaze-obstacle ICS heater).

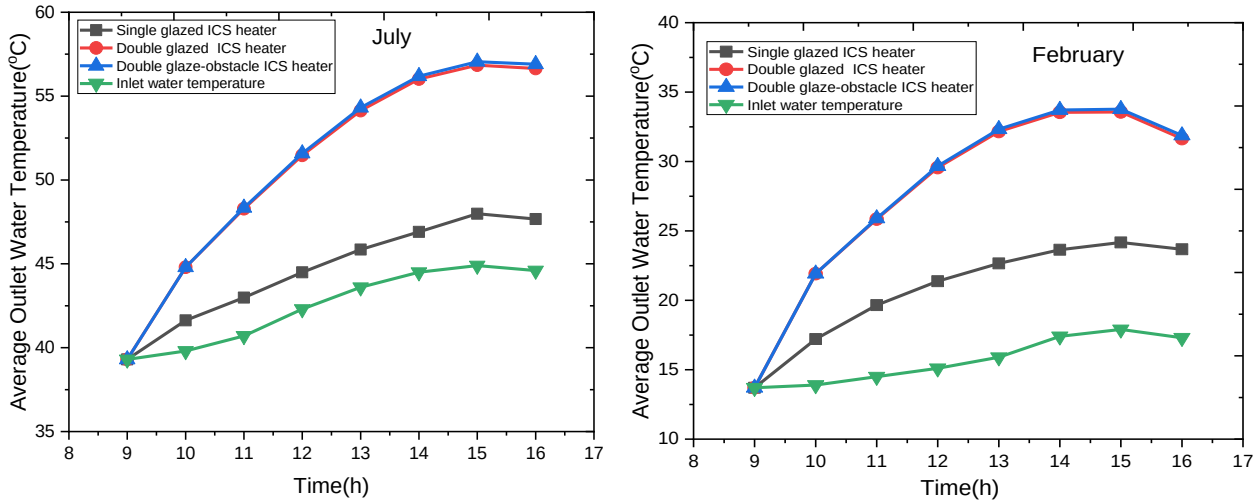

Fig. 6. Variation of average outlet and inlet temperatures for load condition in July and February

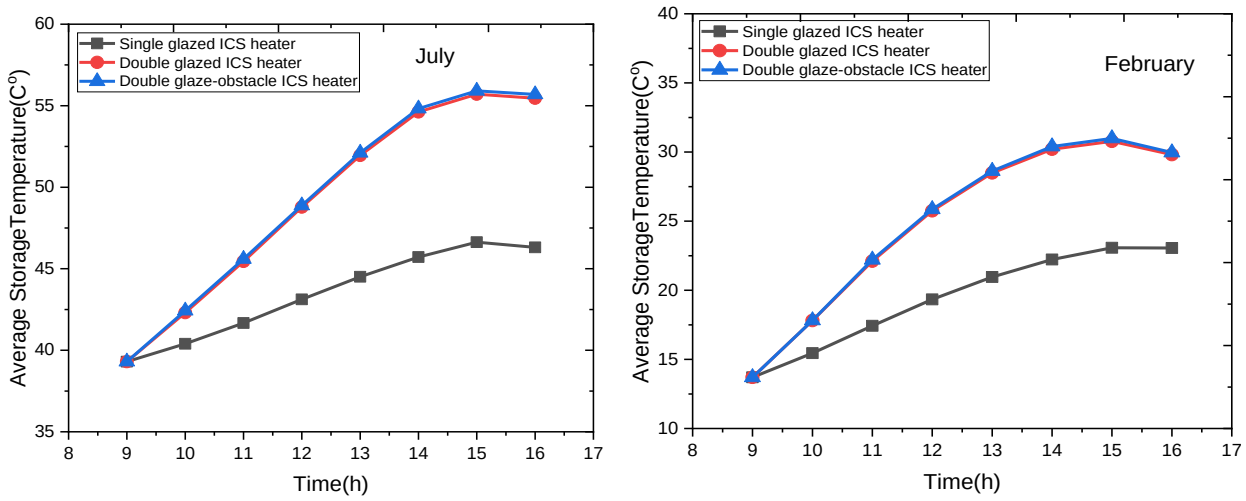

Fig. 7. Variation of average storage temperature for load condition in July and February

4.3 Streamlines Patterns

Three dimensional simulations make a detailed description of the convection motion of water inside the heaters and visualize of streamlines tracks obviously. Figure 8 shows streamlines distribution in the three ISC heaters at 15 p.m. during February. It is observed that, a result of temperature increasing the velocity increases also. Due to buoyancy forces effect. The fluid in contact with the hot inclined surface rises. Some of fluid turn towards the interior of heater because they don't have enough energy to keep upward motion. As it can be seen in this figure, one main circulation cell (vortexes) exists within the (single glazed ICS heater) and (double glazed ICS heater) while more than one cell can be observed in the (double glaze-obstacle ICS heater) because of presence of obstacle.

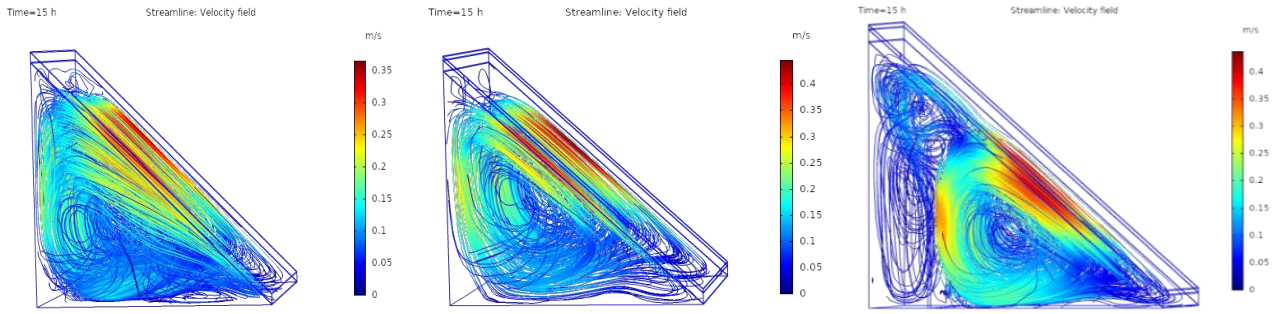

Fig. 8. Streamlines distribution for the three ICS heaters at 15 P.M in February

4.4 Temperature Distribution

Three dimensional view of temperature distribution through three ISC heaters under study are shown in Figure 9 study at 15 p.m. during February. Significant thermal gradients inside the volume of water can be noted. The solar radiation absorbed prompts heat transfer throughout the heater at a resulting of change in fluid density. As a result, buoyancy effect induces natural circulation of the fluid relative to the heater solid surface. For a continuous heat influx, the process is continuous. As can be seen, the (double glaze-obstacle ICS heater) recorded the highest temperature.

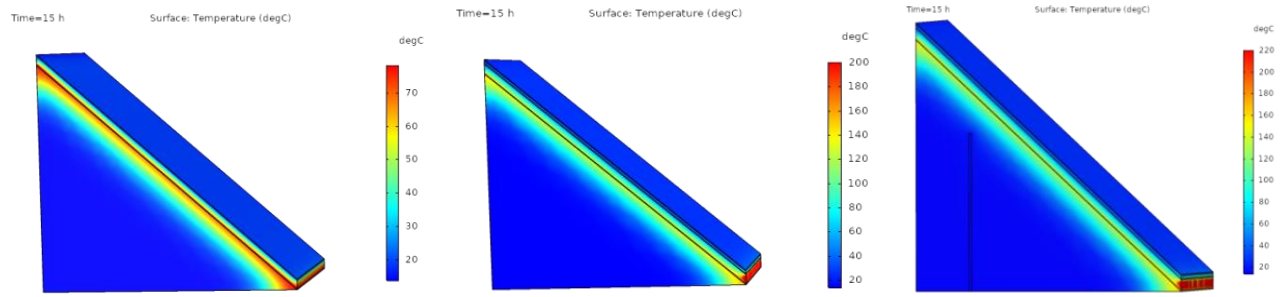

Fig. 9. Temperature distributions for the three ICS heaters at 15 P.M in February

4.5 Performance ICS Heaters

4.5.1 Useful energy

Heat gain is dependent on the variance of the mean storage temperature over the operation time. Eq. (13) and Eq. (14) allow for the evaluation of the useful energy for no load and load condition. Figure 10 and Figure 11 show the average variation of the hourly useful energy for the three ISC heaters during the operation period for no-load and load condition respectively. It is noted that the useful energy reaches its maximum value and then decrease after 13 p.m. in February and but after 14 p.m. in July for no-load and load case. When there was a load, higher levels of the useful energy were seen than when there was no load case. The maximum value was only 2128.48 W in February, whereas the highest value was 1973.17 W in July for the (double glaze-obstacle ICS heater).

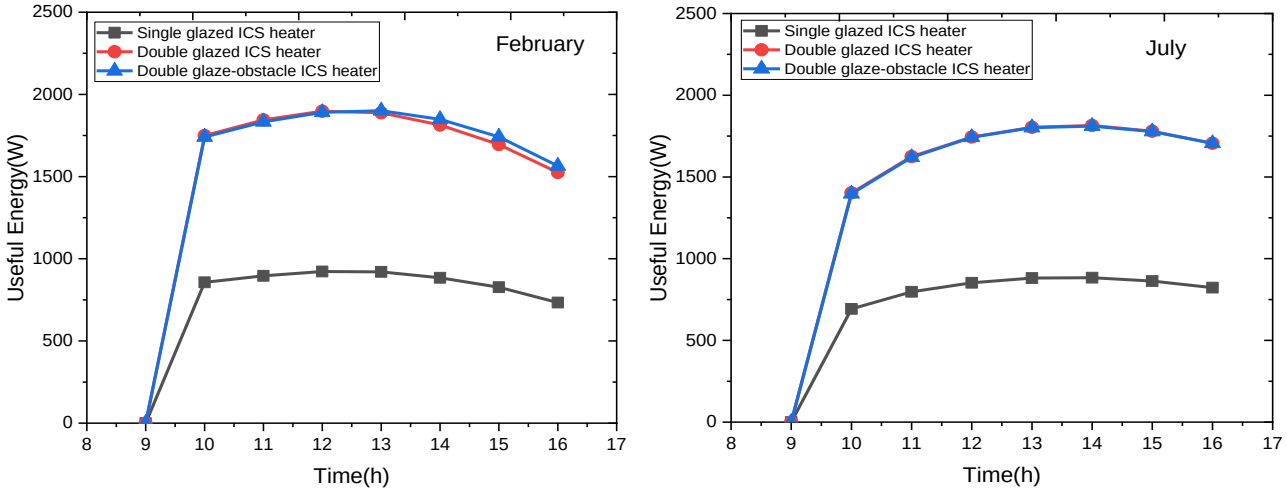

Fig. 10. Variation of the useful energy for the three ICS heaters: without load

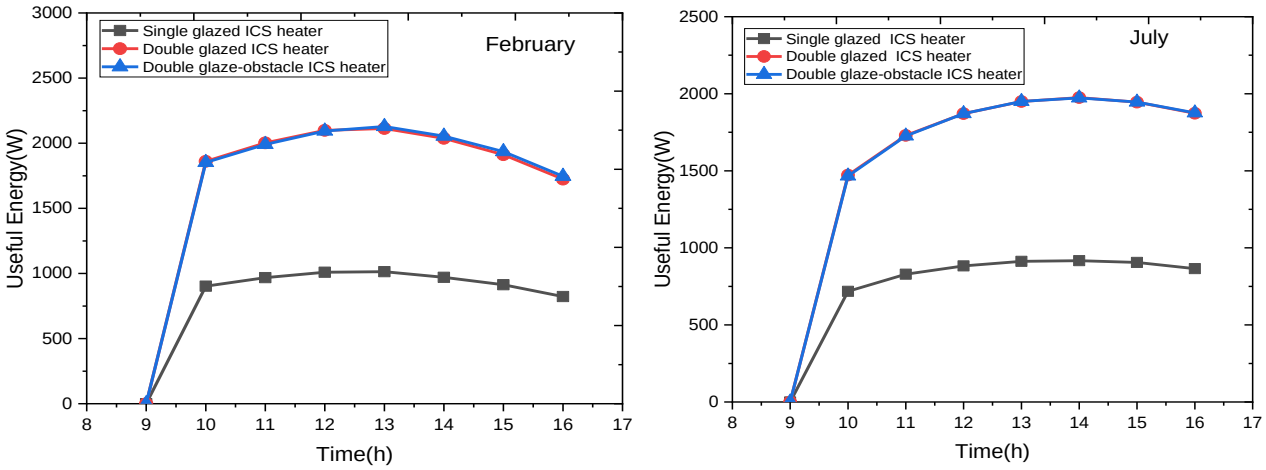

Fig. 11. Variation of the useful energy for the three ICS heaters: with load

4.5.2 Hourly and overall thermal efficiency

Figure 12 and Figure 13 show the average hourly variation of instantaneous thermal efficiency for the three ISC heaters during the operation period for load and no-load conditions. The variation of instantaneous efficiency follows closely the variation of useful transferred energy. During the early daylight, the ICS heaters efficiency is low because the falling solar radiation is small. Then as the incident solar radiation increases, heater efficiency increases until midday because of the rise in the heater water temperature and low heat loss. After that, the efficiency is returned decreasing because of the reduction in the thermal energy accumulated as a result of heat loss. The maximum value of instantaneous efficiency for the (double glaze-obstacle ICS heater) are of 59.95 % at 13 P.M. in February for load case. The average daily overall efficiency for the three ICS heaters in cases of no-load and load conditions in February and July is depicted in Figure (14). It was found that the (single glazed ICS heater) total efficiency is lower than the total efficiency of the other heaters. Under load conditions, the (double glaze-obstacle ICS heater) and (double glazed ICS heater) had a higher overall efficiency than the (single glazed ICS heater) with a maximum a value of 48.92% in February. Generally, the total efficiency under no-load conditions is lower than load.

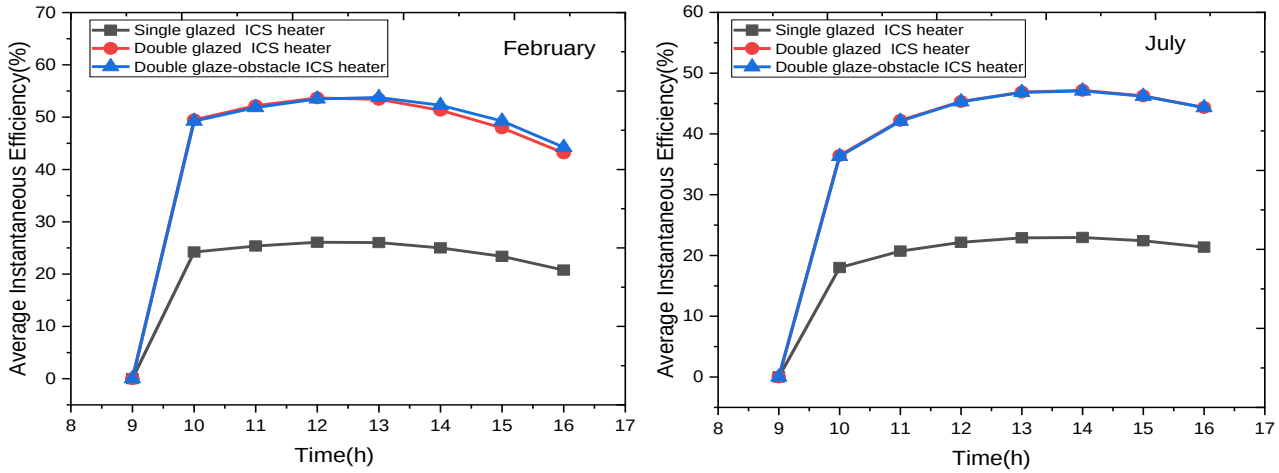

Fig. 12. Variation of the average instantaneous efficiency of three ICS heaters: without load

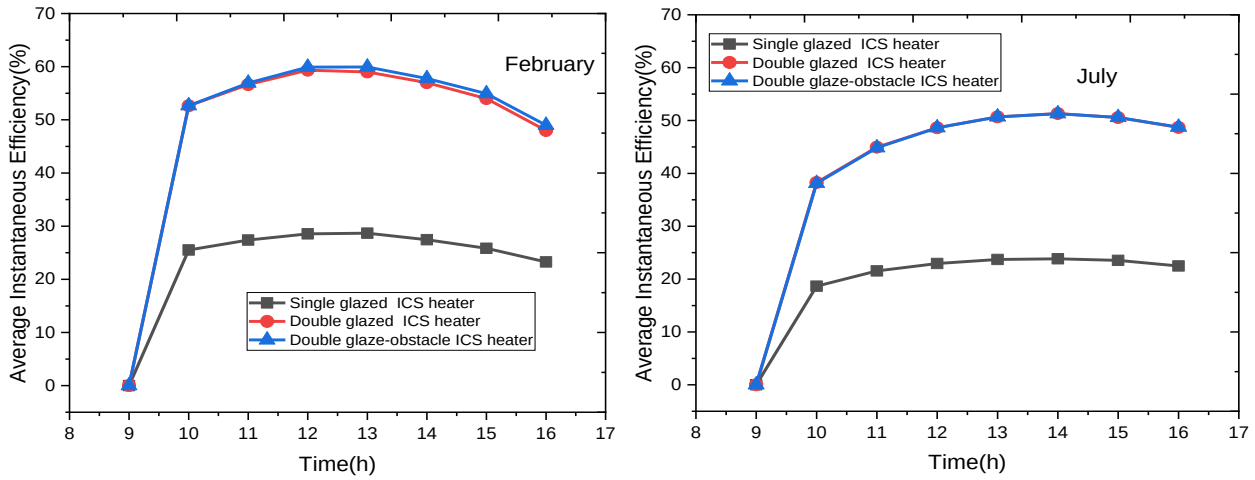

Fig. 13. Variation of the average instantaneous efficiency of three ICS heaters: with load

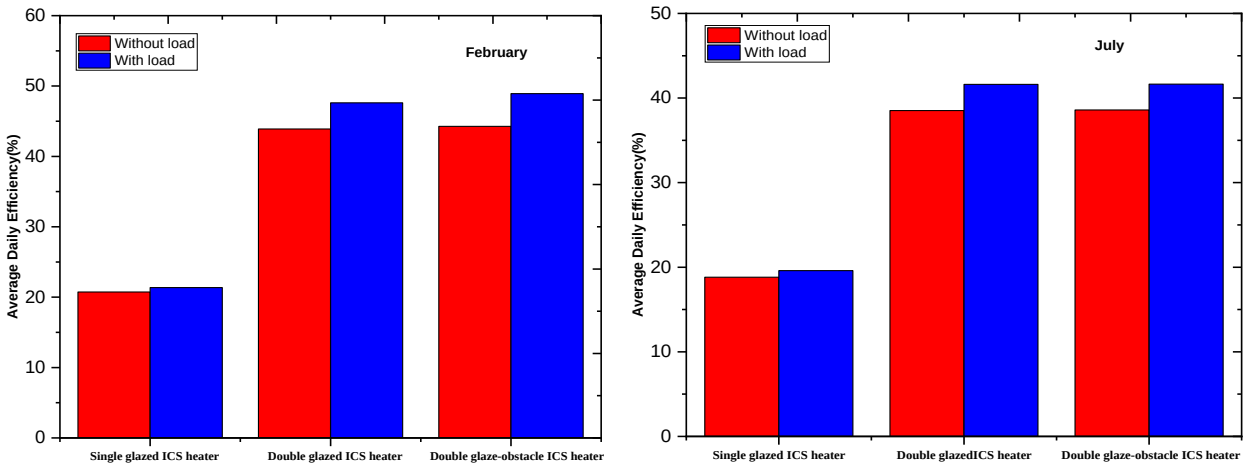

Fig. 14. Variation of the average overall efficiency of three ICS heaters

4.6 Heat Transfer

This section investigates the effect of addition the glass cover above a (single glazed ICS heater). Addition a glass cover causes an increase in the temperature of all heater components because the decrease in the heat transfers though the ambient. Figure 15 shows the variation of average Nusselt number and the convective heat transfer coefficient in the closed air space for different values of Rayleigh number for all ICS heaters. From the results, it is seen that the average Nusselt number and heat transfer coefficient increases as the Rayleigh number increases for all cases. Also, the presence of additional glass cover leads to a decrease in average Nusselt number and heat transfer between the absorber plate and confined air and this reflecting in a higher storage water temperature.

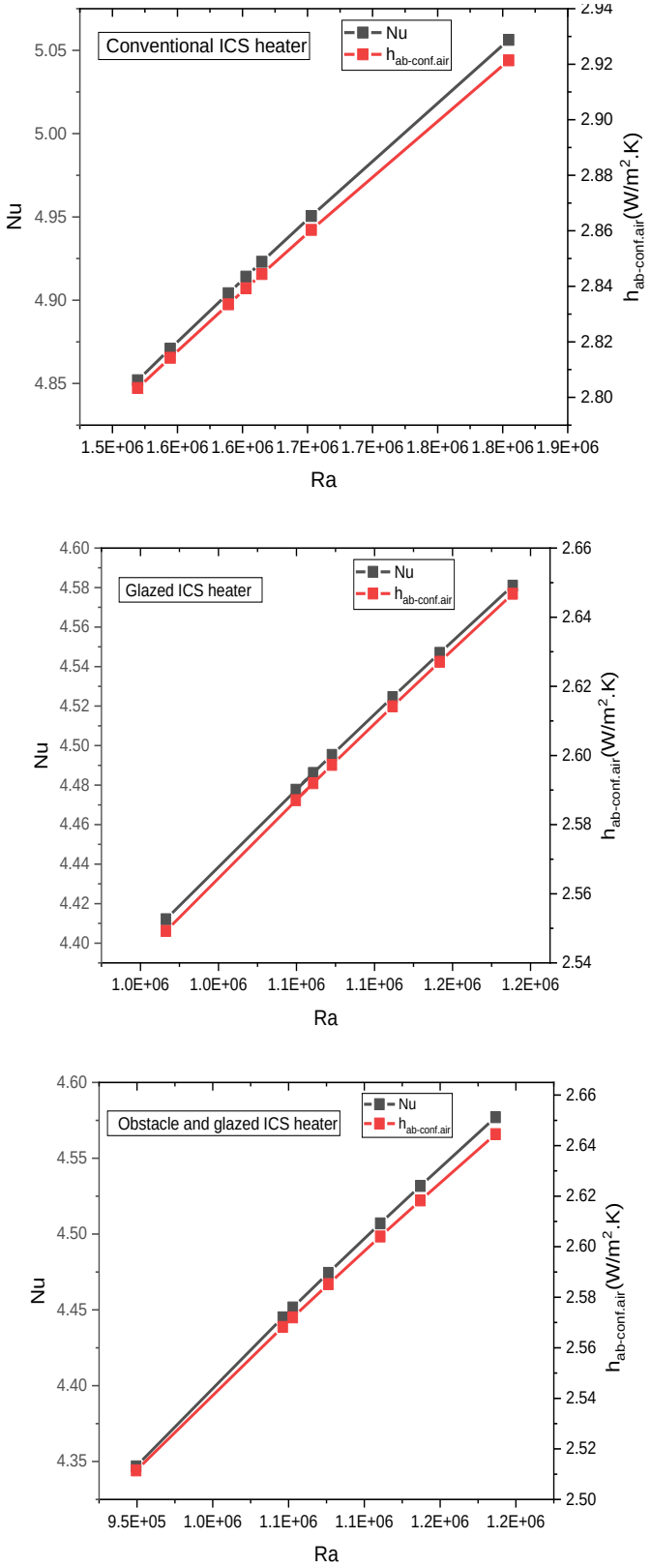

Fig. 15. Variation of Nusselt number and heat transfer coefficient with Rayleigh number for the three ICS heaters

4.7 Effect of Obstacle Dimensions

Effects of using an obstacle inside of heater to disrupt circulation of the water and effect of this circulation on the storage water temperature distribution is determined inside the (double glaze-obstacle ICS heater). This was done by using three different length ratios of the obstacle, h/W=0.2, 0.3, 0.4, 0.5, 0.6 with the following selected distance and obstacle thickness ratios, x/W =0.1, 0.2, 0.3, tw/W=0.01, 0.015, 0.02, 0.025 respectively and was presented in Figure 16. All calculations were performed in February. It can be seen when raising the obstacle length (h) and obstacle distance (x) no impact on the storage temperature was seen until 14 P.M and maximum temperature value was found at (h/W=0.6 and x/W=0.1, 0.2). The water temperature gives nearly the same value for the presented values of (tw/W).

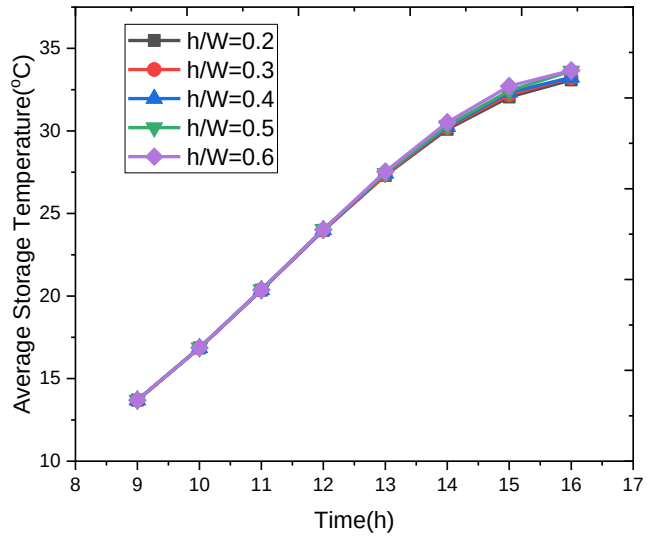

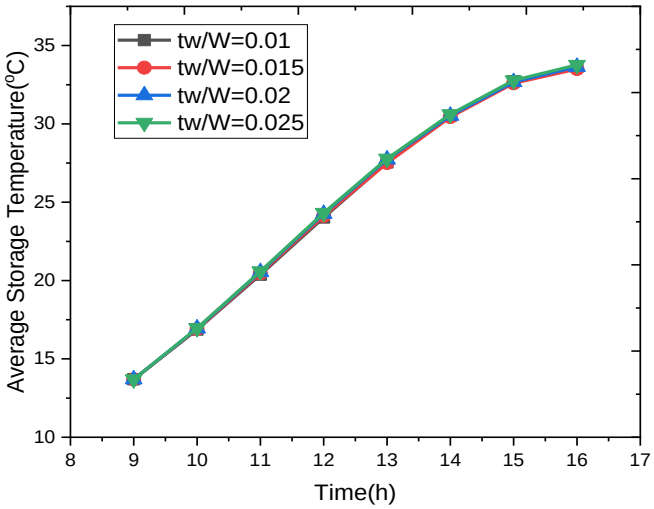

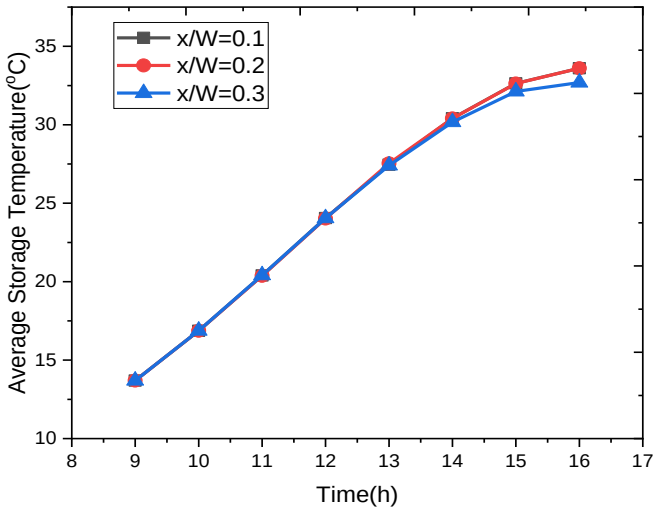

Fig. 16. Effect of the obstacle dimensions on storage water temperature for the (double glaze-obstacle ICS heater): without load

5. Conclusions

A numerical CFD has been developed to study the heat transfer and fluid flow inside three ICS heaters. The results showed when there is no load, and until the end of the operating period, the mean storage temperature is increased with time. The double glaze-obstacle ICS heater storage temperature can reach a maximum value of 61.02 °C in July when the tap water temperatures was 39.3 °C, while for load conditions, the maximum difference between outlet and inlet water temperatures are 15.87 ° C in February at 3 P.M. For load conditions, the double glaze-obstacle ICS and double glazed ICS heater generally had a higher overall efficiency and useful energy than the single glazed ICS heater with a maximum value of 48.92% and 2128.48 W respectively in February. Moreover, the average Nusselt number and heat transfer between the absorber plate and confined air decreases and this reflecting in a higher storage water temperature. Finally, the presence of obstacle inside ICS heater had a little increase in the performance of double glazed ICS heater.

Acknowledgement

This research was not funded by any grant.

References

[1] Çomaklı, Kemal, Uğur Çakır, Mehmet Kaya, and Kadir Bakirci. "The relation of collector and storage tank size in solar heating systems." *Energy Conversion and Management* 63 (2012): 112-117. https://doi.org/10.1016/j.enconman.2012.01.031

[2] Bakirci, Kadir. "A simple calculation method for estimation of instantaneous global solar radiation on horizontal surface." *Journal of Thermal Science and Technology* 29, no. 2 (2009): 53-58.

[3] Bakirci, Kadir. "Correlations for estimation of daily global solar radiation with hours of bright sunshine in Turkey." *Energy* 34, no. 4 (2009): 485-501. https://doi.org/10.1016/j.energy.2009.02.005

[4] Pandya, Himanshu, and Arun Kumar Behura. "Experimental study of V-through solar water heater for tilt angle and glass transmissivity." *Energy Procedia* 109 (2017): 377-384. https://doi.org/10.1016/j.egypro.2017.03.034

[5] Bakirci, Kadir, Omer Ozyurt, Kemal Comakli, and Omer Comakli. "Energy analysis of a solar-ground source heat pump system with vertical closed-loop for heating applications." *Energy* 36, no. 5 (2011): 3224-3232. https://doi.org/10.1016/j.energy.2011.03.011

[6] Comakli, Omer, Kemal Comakli, Nesrin Ozdemir, and Mehmet Yilmaz. "Analysis of heat pumps with zeotropic refrigerant mixtures by Taguchi method." *Journal of Thermal Science and Technology* 30 (2010): 113-122.

[7] Dehghan, A. A., and A. Barzegar. "Thermal performance behavior of a domestic hot water solar storage tank during consumption operation." *Energy Conversion and Management* 52, no. 1 (2011): 468-476. https://doi.org/10.1016/j.enconman.2010.06.075
[8] Ahmed, Omer Khalil. "Experimental and numerical investigation of cylindrical storage collector (case study)." *Case Studies in Thermal Engineering* 10 (2017): 362-369. https://doi.org/10.1016/j.csite.2017.09.003
[9] Mohammed, Suha Abdulelah. "An Experimental Study on Improving the Thermal Storage of ICWS." *International Journal of Scientific & Engineering Research* 5, no. 9 (2014).
[10] Ahmed, Omer Khalil, and A. H. Ahmed. "Principle of Renewable energies." *Baghdad: Foundation of Technical Education* (2011).
[11] Majeed Ali, Obiad, Ahmed Hassen Ahmed, and Omer Khalil Ahmad. "Effect of the Shape Surface of Absorber Plate on Performance of Built-In-Storage Solar Water Heater." *Iraqi Journal of Desert Studies* 2, no. 2 (2010): 69-80. https://doi.org/10.36531/ijds.2010.14587
[12] Garg, H. P. "Year round performance studies on a built-in storage type solar water heater at Jodhpur, India." *Solar Energy* 17, no. 3 (1975): 167-172. https://doi.org/10.1016/0038-092X(75)90055-9
[13] Sodha, M. S., J. K. Nayak, S. C. Kaushik, S. P. Sabberwal, and M. A. S. Malik. "Performance of a collector/storage solar water heater." *Energy Conversion* 19, no. 1 (1979): 41-47. https://doi.org/10.1016/0013-7480(79)90015-9
[14] Nahar, N. M., and K. S. Malhotra. "A low cost collector-cum-storage type solar water heater." *International Journal of Energy Research* 6, no. 2 (1982): 195-198. https://doi.org/10.1002/er.4440060211
[15] Abd-Alghani, H. "Domestic solar water heater." *M. Sc. Thesis, Mechanical Engineering Department, University of Basra*, 1983.
[16] Garg, H. P., and Usha Rani. "Theoretical and experimental studies on collector/storage type solar water heater." *Solar Energy* 29, no. 6 (1982): 467-478. https://doi.org/10.1016/0038-092X(82)90055-X
[17] Khalifa, Abdul-Jabbar N., and M. M. Mehdi. "On the verification of one dimensional heat flow in a horizontal thermosyphon storage tank." *Energy Conversion and Management* 40, no. 9 (1999): 961-974. https://doi.org/10.1016/S0196-8904(98)00150-2
[18] Farhan, A. "Computational model for a prism shaped storage solar collector with a right triangular cross section." *M. Sc. Thesis, Mechanical Engineering Department, University of Baghdad*, 2002.
[19] Vaxman, B., and M. Sokolov. "Experiments with an integral compact solar water heater." *Solar Energy* 34, no. 6 (1985): 447-454. https://doi.org/10.1016/0038-092X(85)90018-0
[20] Joudi, K. A., I. A. Hussein, and A. A. Farhan. "Computational model for a prism shaped storage solar collector with a right triangular cross section." *Energy Conversion and Management* 45, no. 3 (2004): 391-409. https://doi.org/10.1016/S0196-8904(03)00153-5
[21] Pandya, Himanshu, and Arun Kumar Behura. "Experimental study of V-through solar water heater for tilt angle and glass transmissivity." *Energy Procedia* 109 (2017): 377-384. https://doi.org/10.1016/j.egypro.2017.03.034
[22] Ahmad, Omer Khalil, Ahmed Hassan Ahmed, and Obiad Majeed Ali. "Effect of the shape surface of absorber plate on performance of built-in-storage solar water heater." *Journal of Iraqi Desert Studies* 2, no. 2 (2010): 69-80. https://doi.org/10.36531/ijds.2010.14587
[23] Ambarita, Himsar, R. E. T. Siregar, A. D. Ronowikarto, and E. Y. Setyawan. "Effects of the inclination angle on the performance of flat plate solar collector." In *Journal of Physics: Conference Series*, vol. 978, no. 1, p. 012097. IOP Publishing, 2018. https://doi.org/10.1088/1742-6596/978/1/012097
[24] Abdullah, Amani H., Omer K. Ahmed, and Zaid H. Ali. "Performance analysis of the new design of photovoltaic/storage solar collector." *Energy Storage* 1, no. 5 (2019): e79. https://doi.org/10.1002/est2.79
[25] Mokhlif, Nassir D., Muhammad Asmail Eleiwi, and Tadahmun A. Yassen. "Experimental evaluation of a solar water heater integrated with a corrugated absorber plate and insulated flat reflectors." *AIMS Energy* 11, no. 3 (2023): 522-539. https://doi.org/10.3934/energy.2023027
[26] Chandra, Yogender Pal, and Tomas Matuska. "Numerical prediction of the stratification performance in domestic hot water storage tanks." *Renewable Energy* 154 (2020): 1165-1179. https://doi.org/10.1016/j.renene.2020.03.090
[27] Mokhlif, Nassir D., Muhammad Asmail Eleiwi, and Tadahmun Ahmed Yassen. "Experimental investigation of a double glazing integrated solar water heater with corrugated absorber surface." *Materials Today: Proceedings* 42 (2021): 2742-2748. https://doi.org/10.1016/j.matpr.2020.12.714
[28] Yassen, Tadahmun A., Nassir D. Mokhlif, and Muhammad Asmail Eleiwi. "Performance investigation of an integrated solar water heater with corrugated absorber surface for domestic use." *Renewable Energy* 138 (2019): 852-860. https://doi.org/10.1016/j.renene.2019.01.114
[29] Çomaklı, K., U. Çakır, M. Kaya, and B. Sahin. "Energetic and exergetic analysis of a water heating system using solar energy." In *Proceedings of the 5th International Ege Energy Symposium and Exhibition (IEESE-5)*. 2010.
[30] Alizadeh, Shahab. "An experimental and numerical study of thermal stratification in a horizontal cylindrical solar storage tank." *Solar Energy* 66, no. 6 (1999): 409-421. https://doi.org/10.1016/S0038-092X(99)00036-5

[31] Buchberg, H., Ivan Catton, and D. K. Edwards. "Natural convection in enclosed spaces-a review of application to solar energy collection." *ASME Journal of Heat and Mass Transfer* 98, no. 2 (1976): 182-188. https://doi.org/10.1115/1.3450516
[32] Hassan, Hawraa Fadhel Abd. "Experimental Study and Evaluation of Single Slope Solar Still Combined with Parabolic Trough Using Nanofluid." *M. Sc. Thesis, Al-Furat Al-Awsat Technical University*, 2022.
[33] Koffi, P. M. E., H. Y. Andoh, P. Gbaha, S. Touré, and G. Ado. "Theoretical and experimental study of solar water heater with internal exchanger using thermosiphon system." *Energy Conversion and Management* 49, no. 8 (2008): 2279-2290. https://doi.org/10.1016/j.enconman.2008.01.032
[34] COMSOL, AB. "Comsol Multiphysics Reference Manual Version: Comsol 5.1." *COMSOL AB: Stockholm, Sweden* (2015).
[35] Kadhum, Ali Abdul. "Investigation The Performance Of Hybrid Photovoltic/Thermal Solar System Using Nano-Fluid." *PhD Diss., University of Kerbala*, 2019.
[36] Swinbank, W. C. "Long-wave radiation from clear skies." *Quarterly Journal of the Royal Meteorological Society* 89, no. 381 (1963): 339-348. https://doi.org/10.1002/qj.49708938105
[37] Saleh, Noah Mohammed. "Theoretical and practical investigation of the CTPTC performance using FUZZY logic control." *NTU Journal of Renewable Energy* 2, no. 1 (2022): 27-33.
[38] Saeed, Muntadher Mohammed Ali, Dhafer Manea Hachim, and Hassanain Ghani Hameed. "Numerical investigation for single slope solar still performance with optimal amount of Nano-PCM." *Journal of Advanced Research in Fluid Mechanics and Thermal Sciences* 63, no. 2 (2019): 302-316.
[39] Al-Jubori, Omer Khalil Ahmed. "Numerical and Experimental Performance Analysis for a Novel Design of Storage Solar Collector." *PhD diss., Nahrain University*, 2006.
[40] Alawi, W. H. "Numerical and experimental study of the solar collector storage pyramidical with right angle." *PhD diss., M. Sc. Thesis, University of Technology*, Baghdad, 2004.
[41] Ahmed, Omer Khalil. "A numerical and experimental investigation for a triangular storage collector." *Solar Energy* 171 (2018): 884-892. https://doi.org/10.1016/j.solener.2018.06.097
[42] Ahmed, Omer Khalil. "Experimental and numerical investigation of cylindrical storage collector (case study)." *Case Studies in Thermal Engineering* 10 (2017): 362-369. https://doi.org/10.1016/j.csite.2017.09.003
[43] Kumar, Rakesh, and Marc A. Rosen. "Integrated collector-storage solar water heater with extended storage unit." *Applied Thermal Engineering* 31, no. 2-3 (2011): 348-354. https://doi.org/10.1016/j.applthermaleng.2010.09.021
[44] Kessentini, Hamdi, and Chiheb Bouden. "Numerical and experimental study of an integrated solar collector with CPC reflectors." *Renewable Energy* 57 (2013): 577-586. https://doi.org/10.1016/j.renene.2013.02.015
[45] Sathyamurthy, Ravishankar, DG Harris Samuel, and P. K. Nagarajan. "Theoretical analysis of inclined solar still with baffle plates for improving the fresh water yield." *Process Safety and Environmental Protection* 101 (2016): 93-107. https://doi.org/10.1016/j.psep.2015.08.010